III. Proposal for Experimental Tests of the BEC Mechanism

1. Quantum Coherence Requirement for the BEC
2. Size Consideration for Active Spots
3. Role of External Stimulations
4. Possible Schematic Designs for Experimental Setups

1. Quantum Coherence Requirement for Deuteron BEC – High Deuteron Density/Loading Required

$$Assume \quad the \quad reqirement \qquad \lambda \geq d$$

$$deBroglie\ Wavelength, \quad \lambda = \frac{h}{m\mathrm{v}}, \quad mc^2 = 1876\ MeV$$

$$Interatomic\ Distance, \quad d = (n)^{-1/3}, \quad n = \frac{N}{V}$$

$$Average\ Energy, \quad \frac{1}{2}m\mathrm{v}^2 = \frac{3}{2}kT, \quad m\mathrm{v} = \sqrt{3kTm}, \quad \lambda = \frac{h}{\sqrt{3kTm}}$$

T(°K)	λ(A°)	v(km/s)
373	0.95	2.12
300	1.03	1.93
273	1.08	1.84
77	2.0	1.0
20	4.0	0.5
4.2	8.7	0.23

- d = 2.45A° for n = 6.8 x 10^{22}cm$^{-3$} • d = 24.5A° for n = 6.8 x 10^{19}cm^{-3}
- If the average D^+ velocity is slower in metals, the effective temperature of mobile D^+'s can be lower than the ambient temperature.

2. Size Consideration for Active Spots

- A sufficient number of Bosons is required for BEC:
  L and N for $n = 6.8 \times 10^{22} cm^{-3}$ ($n=N/V = N/L^3$)

L	N(deuterons)
25nm	10^6
0.25μm	10^9
2.5 μm	10^{12}

- Quantum coherence may be difficult to achieve for the entire volume (L^3) if L is too large

3. Role of External Stimulations

- Attain high density/flux of (D_n^+, e_m^-)
- Cool (D_m^+, e_n^-) in atomic clusters, bubbles, or cavities
- Type/mode
  - Acoustic
  - Electromagnetic Fields
    - » Electric Field (electrolysis, charge discharge, etc.)
    - » Magnetic Fields (affect mostly electrons, electron cooling?)
    - » Lasers (affect mostly electrons, electron cooling?)

4. Schematic Designs for Experimental Setups

A. Vyco Glass, Aerogel, and Carbon Aerogel

B. Designs for Electrolysis Experiments

C. Designs for Gas Experiments

Vycor Glass

VYCOR® Brand Porous Glass 7930

Physical Properties

Approx. Specific Gravity (dry)	1.5
Void Space	28% of Vol.
Internal Surface Area	250m2/gram
Avg. Pore Diameter (Standard)	40 A or 4 x 10e-9 meters
Appearance	opalescent
Avg. Modulus of Rupture of Abraded "A" rods, 25 °C	6000 psi
Young's Elastic Modulus, 25 °C	2.5×10^6 psi
Loss Tangent at 25 °C, 100 Hz	.007*
Dielectric Constant at 25 °C, 100 Hz	3.1*

*Loss Tangent and Dielectric Constant are affected by water in porous glass. The above porous glass sample was activated at 400 °C, cooled in a desiccator, and immediately measured to minimize water pickup.

Composition

SiO_2	96%
B_2O_3	3%
Na_2O	0.40/a
$R_2O_3 \pm RO_2$	<1%

R = Mostly Al_2O_3 and ZrO_2

Aerogel

AEROGEL

CATCHING COMET DUST

Particle captured in Aerogel

AEROGEL QUICK FACTS

It is 99.8% Air

Provides 39 times more insulating than the best fiberglass insulation

Is 1,000 times less dense than glass

Was used on the Mars Pathfinder rover

Aerogel

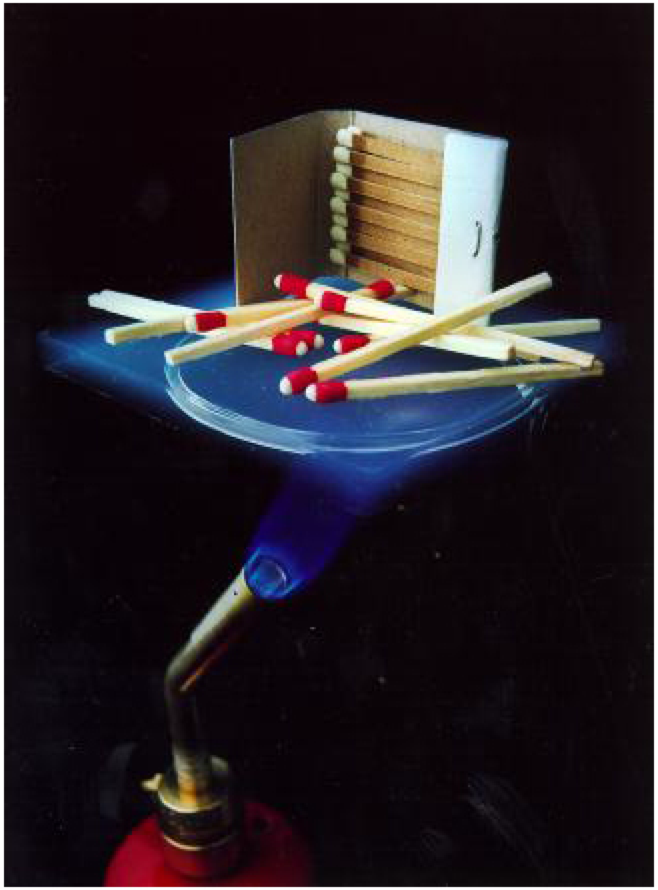

Matches on Aerogel over a Flame

Aerogel Supporting a Brick

Carbon Aerogel

R.W.Pekela et al. in “ Sol Gel Science and Applications” (Plenum, 1994) p. 369

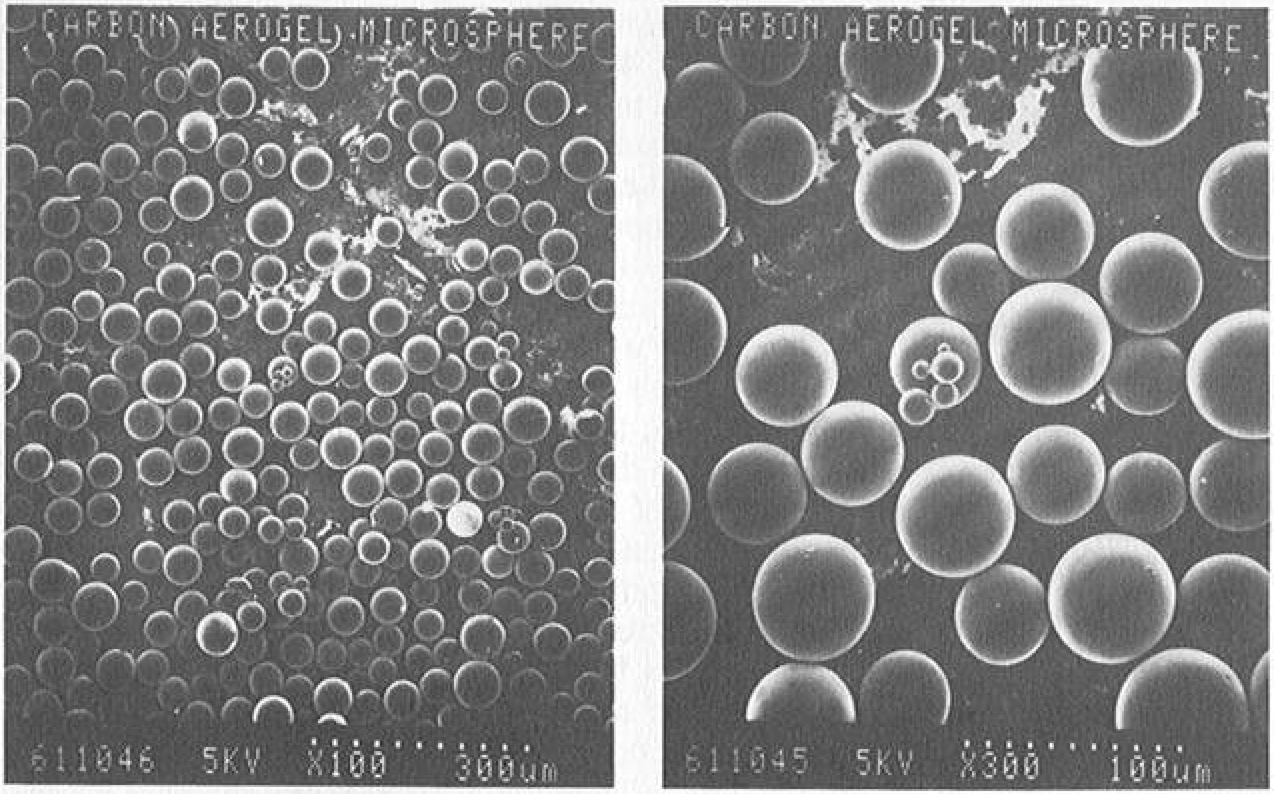

Figure 2. Scanning electron micrographs of carbon aerogel microspheres (~0.8 g/cc; R/C=200; 1050 °C).

A Schematic Design for Electrolysis Experiment

- Cathode (-):
  - Carbon aerogel film on Ni mesh/foil, Ni mesh/foil, or Pd foil
- External electromagnetic fields to be applied for slowing down D+'s (cooling)

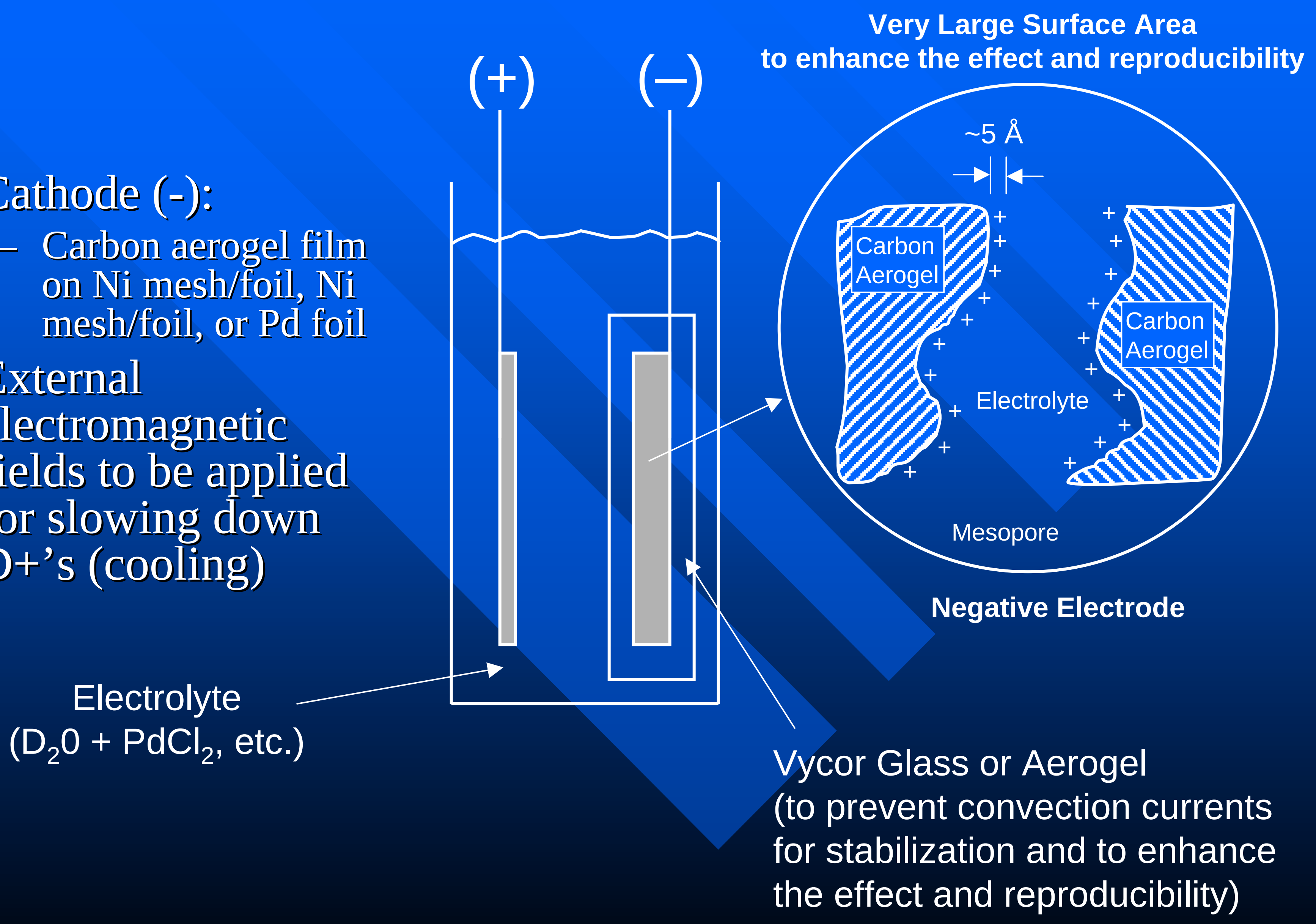

A Schematic Design for D_2 Gas Experiments with Electric Field

- Deterium-Loaded Negative Plate:
  - Carbon aerogel film on Ni mesh/foil, Ni mesh/foil, or Pd foil
- Apply external electromagnetic field to slow down D+'s (cooling) (alternating currents, etc.)

Very Large Surface Area
to enhance the effect and reproducibility

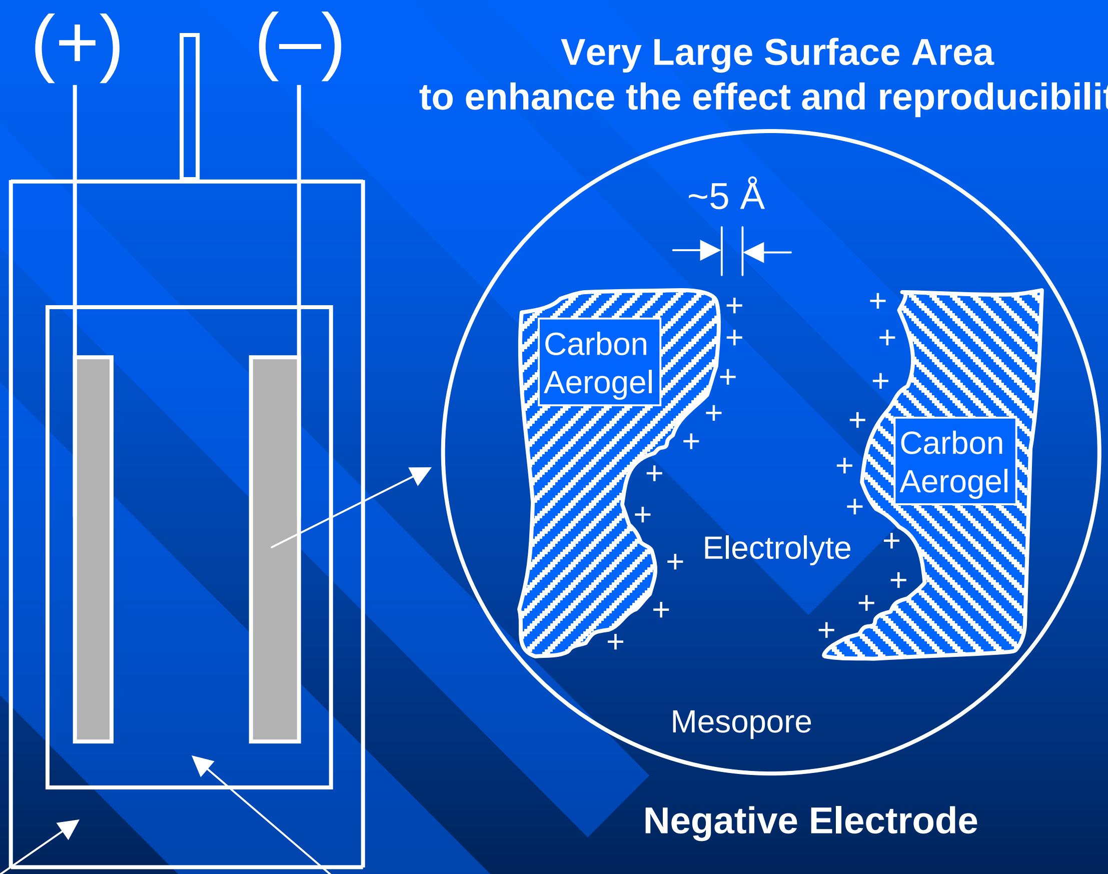

D_2 gas at different temperatures and pressures

Vycor Glass or Aerogel
(to prevent convection currents for stabilization and to enhance the effect and reproducibility)

A Schematic Design for D_2 Gas Experiments

- Apply external electric field, magnetic field, or laser to slow down deuteriums (cooling)

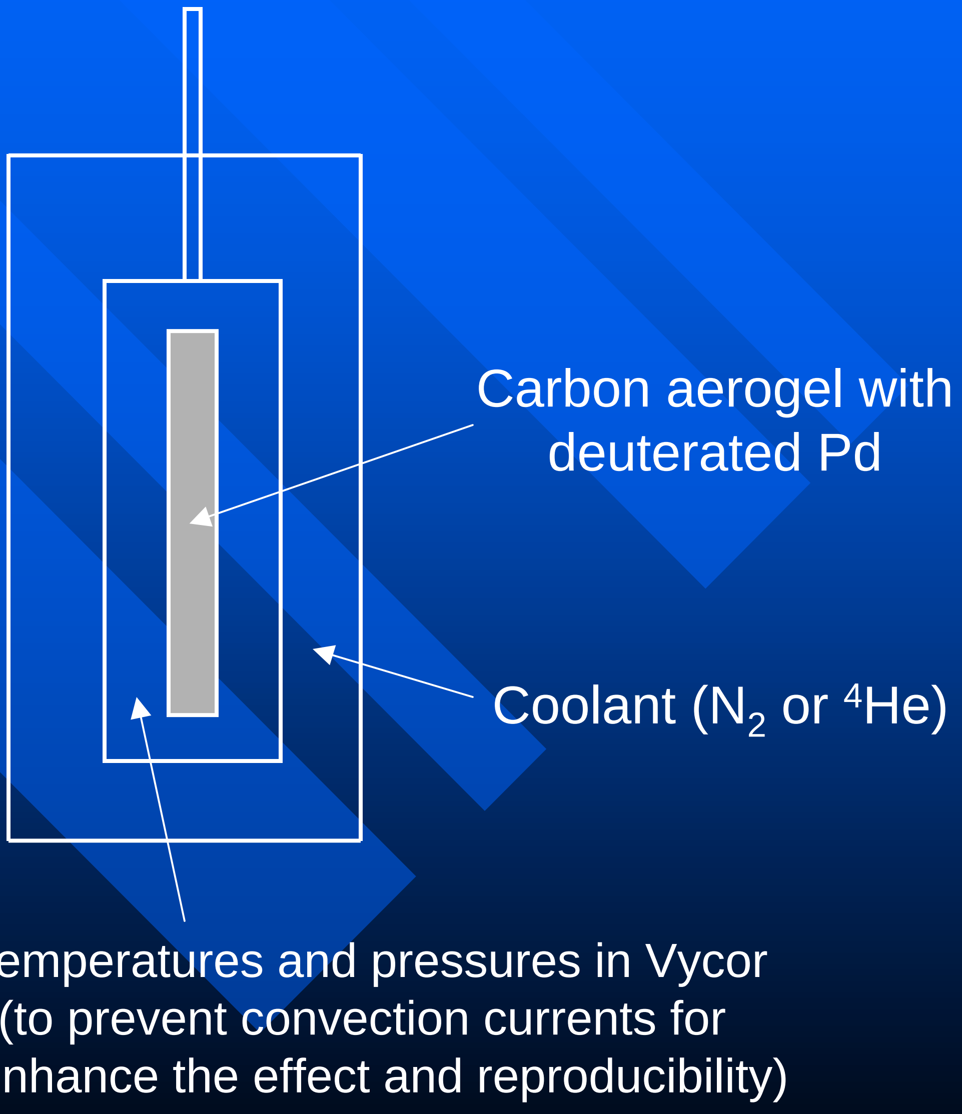

Phase Diagram of Para Hydrogen

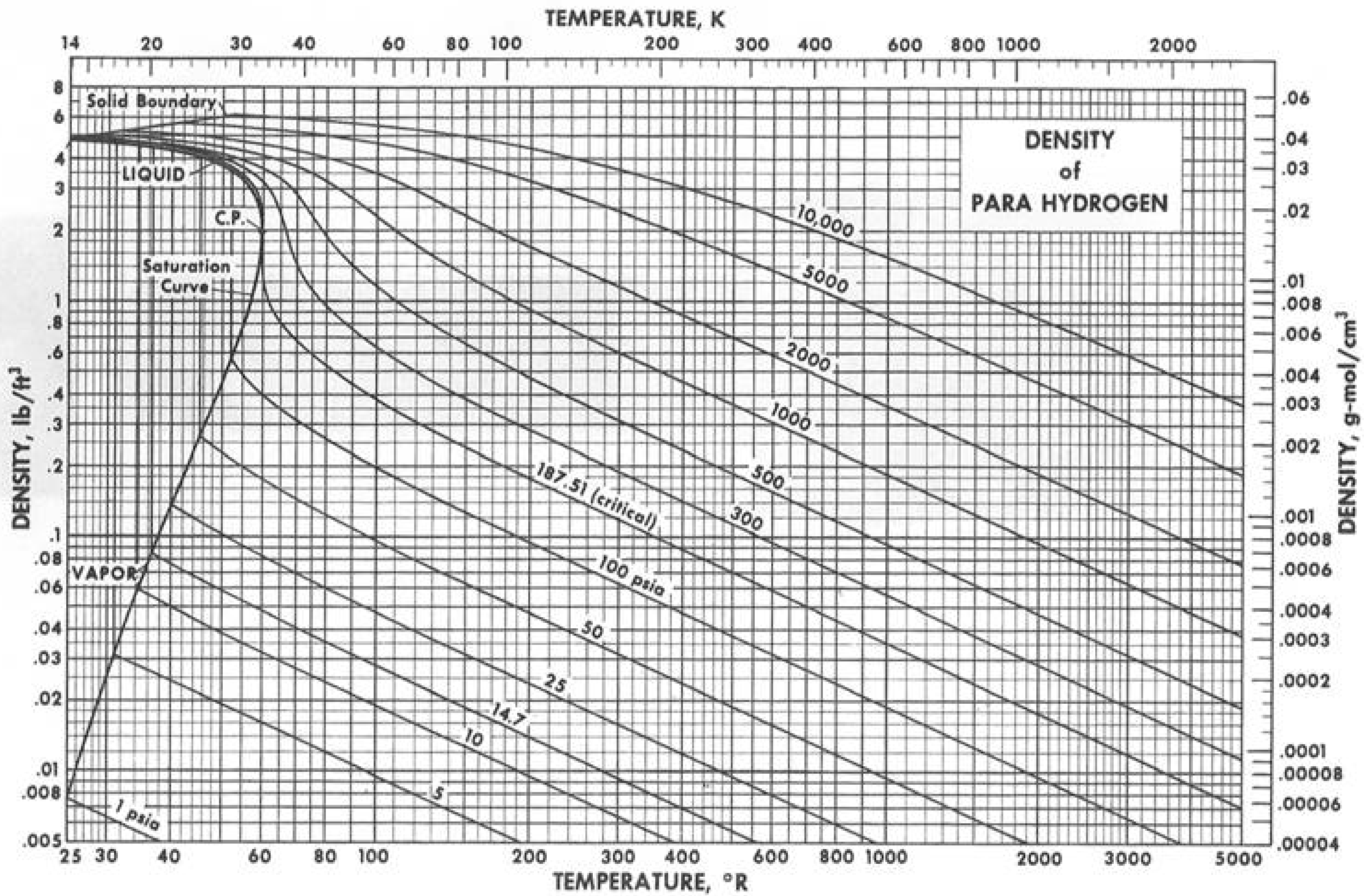

FIGURE 3.15. Density (P-ρ-T).

Summary: Requirements for Design of Experimental Tests of the BEC Mechanism

- Mobile Deuterons:

  (1) Non-equilibrium fluctuations may be able to make vacancies or impurities sufficiently mobile so as to allow Bose nuclei to move collectively in localized regions.

  (2) Provide mobility by external stimulation.

- High Deuteron Density and Low Temperature:

  (3) Average de Broglie wavelength of Bose nuclei should be comparable to or greater than average distance between Bose nuclei, thus providing "Quantum Coherence".

  (4) Provide cooling by external stimulation (electron cooling ?).

  (5) Achieve a high deuteron density by loading and/or pressure.

- Sufficiently Large Number of Deuterons in a Stable Ion Trap:

  (6) Maintain a minimum size for ion traps.

  (7) Maintain an optimal maximum size for ion traps for stability.

  (8) Use Vycor Glass, Aerogel, and/or Carbon Aerogel

  (a) to control optimam sizes of ion traps,

  (b) to maintain stability of the system, and

  (c) to enhance the LENR effects and reproducibility !!!

IV. Generalization to Low Energy Nuclear Transmutation (Kim and Zubarev, ICFF-11)

We consider a mixture of two different positive charged species of bosons, labeled 1 and 2 with N_1 and N_2 particles. Let $Z_1 \geq 0$, $Z_2 \geq 0$ and m_1, m_2 to be charges and masses, respectively. We assume that trapping potentials V_i are isotropic and harmonic

$$V_i(\vec{r}) = m_i \omega_i^2 r^2 / 2. \tag{1}$$

The mean-field energy functional for the two-component system is given by generalization of the one-component case (Y.E. Kim and A.L. Zubarev, Phys. Rev. A**64**, 013603 (2001)).

$$\begin{aligned} E = \sum_{i=1}^{2} \int d\vec{r} [\frac{\hbar^2}{2m_i} \mid \nabla \psi_i \mid^2 + V_i \mid \psi_i \mid^2] \\ + \frac{e^2}{2} \int d\vec{r} d\vec{r'} \frac{(Z_1 n_1(\vec{r}) + Z_2 n_2(\vec{r}))(Z_1 n_1(\vec{r'}) + Z_2 n_2(\vec{r'}))}{\mid \vec{r} - \vec{r'} \mid}, \end{aligned} \tag{2}$$

where n_i denotes density of species i, $\mid \psi_i \mid^2 = n_i$,

$$\int d\vec{r} n_i(\vec{r}) = N_i. \tag{3}$$

In Eq.(2) we neglect effects of order $\frac{1}{N_i}$.

The minimization of the functional, Eq.(2), with subsidiary conditions, Eq.(3), leads to the following time-independent mean-field equations

$$\frac{\hbar^2}{2m_1}\nabla^2\psi_1(\vec{r}) + V_1\psi_1(\vec{r}) + e^2\int\frac{d\vec{r'}}{\mid\vec{r}-\vec{r'}\mid}[Z_1^2 n_1(\vec{r'}) + Z_1 Z_2 n_2(\vec{r'})]\psi_1(\vec{r}) = \mu_1\psi_1(\vec{r}),$$

$$\frac{\hbar^2}{2m_2}\nabla^2\psi_2(\vec{r}) + V_2\psi_2(\vec{r}) + e^2\int\frac{d\vec{r'}}{\mid\vec{r}-\vec{r'}\mid}[Z_2^2 n_2(\vec{r'}) + Z_1 Z_2 n_1(\vec{r'})]\psi_2(\vec{r}) = \mu_2\psi_2(\vec{r}),$$

(4)

where μ_i are chemical potentials, which are related to the ground-state energy, Eq.(2) by the general thermodynamics identity

$$\mu_i = \frac{\partial E}{\partial N_i}. \tag{5}$$

We note that the mean-field theory, Eqs. (4) and (5), cannot describe the Wigner-crystallization regime (E.P. Wigner, Phys. Rev. **46**, 1002 (1934)).

In the Thomas-Fermi (TF) approximation, in which one neglects the kinetic energy terms in Eqs.(4), which then become

$$\mu_1 = V_1 + e^2 \int \frac{d\vec{r'}}{|\vec{r} - \vec{r'}|}[Z_1^2 n_1(\vec{r'}) + Z_1 Z_2 n_2(\vec{r'})],$$
$$\mu_2 = V_2 + e^2 \int \frac{d\vec{r'}}{|\vec{r} - \vec{r'}|}[Z_2^2 n_2(\vec{r'}) + Z_1 Z_2 n_1(\vec{r'})]. \qquad (6)$$

Equations (6) hold in the region where n_i are positive and $n_i = 0$ outside this region.

We can obtain from these equations that

$$\mu_2 - \frac{Z_2}{Z_1}\mu_1 = (\frac{m_2\omega_2^2}{m_1\omega_1^2} - \frac{Z_2}{Z_1})\frac{m_1\omega_1^2}{2}r^2, \qquad (7)$$

therefore we have proved that Eqs. (6) have nontrivial solution if and only if

$$\lambda = \frac{m_2\omega_2^2 Z_1}{m_1\omega_1^2 Z_2} = 1, \qquad (8)$$

in this case $\mu_2 = \frac{Z_2}{Z_1}\mu_1$

Eqs. (6) can be solved analitycally

$$n_i(\vec{r}) = \frac{3N_i}{4\pi R_i^3}\theta(R_i^2 - r^2), \tag{9}$$

where θ denotes the unit positive step function,

$$\begin{aligned} R_1 &= \sqrt{\frac{\hbar}{m_1\omega_1}}[\gamma_c^{(1)}(Z_1^2 N_1 + Z_1 Z_2 N_2)]^{1/3}, \\ R_2 &= \sqrt{\frac{\hbar}{m_2\omega_2}}[\gamma_c^{(2)}(Z_2^2 N_2 + Z_1 Z_2 N_1]^{1/3}, \end{aligned} \tag{10}$$

and $\gamma_c^{(i)} = \alpha\sqrt{m_i c^2/(\hbar\omega_i)}$.

$R_1 = R_2$ for $\lambda = 1$.

Straightforward calculations with n_i from Eqs. (9) yeld

$$\mu_i = \frac{3}{2} m_i \omega_i^2 R_i^2, \tag{11}$$

and

$$E = \frac{9}{10} \frac{\hbar\omega_1}{Z_1^2} [\gamma_c^{(1)}]^{2/3} [(Z_1^2 N_1 + Z_1 Z_2 N_2)]^{5/3}. \tag{12}$$

Comparing radii of clouds R_1 and R_2, Eqs.(10), we see that $R_1 = R_2$, therefore we found that depending of the ratio λ, Eqs.(8), the two components coexist in the same region of space, despite the Coulomb repulsion between two species.

This result is obtained in the TF approximation, Eqs.(6). If $\lambda = 1$, and $N_i \gg 1$, $\gamma_c^{(i)} N_j \gg 1$, the TF approximation provides an accurate description of the exact mean-field solution (except a narrow region near a surface).

For a general value of λ, the mixture becomes unstable against deviations from uniformity. Although the TF approximation is not applicable for this case we, nevertheless, expect that if $\lambda \approx 1$ and $N_i \gg 1$, $\gamma_c^{(i)} N_j \gg 1$, the two component may coexist in same regions of space.

Example:

If we assume $\omega_1 = \omega_2$, we have from Eq.(8)

$$\lambda = m_2 Z_1/(m_1 Z_2) = 1$$

or

$$Z_1/Z_2 = m_1/m_2 \approx (Z_1 + \tilde{N}_1)/(Z_2 + \tilde{N}_2),$$

where $\tilde{N}_i$ is the number of neutrons in the Bose nuclear specie i.

"UNFORTUNATELY THIS LAB IS FUNDED ONLY BY AS MUCH <u>GOLD</u> AS WE CAN MAKE FROM LEAD."